

Three-Dimensional Endwall Disturbances in
the Entrance Region of a Supersonic Cascade

H. A. Schreiber

Institut für Antriebstechnik
DFVLR Köln
Postfach 90 60 58
5000 Köln 90, FR Germany

Summary

Unexpected discrepancies in the blade suction surface Mach number distribution of a supersonic compressor blade section with low aspect ratio (0.9) initiated a test program to investigate the flow field in the cascade entrance region. Using a laser transit anemometer, the flow field near the blade suction surface was analysed in spanwise direction. The measurements showed expansion and weak shock waves emanating from the corner region where the blade leading edge enters the wind tunnel endwall boundary-layer. It is assumed, that these disturbances are induced by a complex interaction mechanism of the detached bow shock wave in front of the blade leading edge with the endwall boundary-layer. The detected expansion and compression waves attenuate towards the wind tunnel center, however, the blade pressure distribution and eventually the blade performance in the mid-span region can be influenced, especially if the cascade tests are performed with blades of low aspect ratio.

Nomenclature

b blade span
 l chord length
 M Mach number
 M_{is} isentropic Mach number using upstream total pressure
 SS blade suction surface
 t_{LE} leading edge thickness
 x/b dimensionless chordwise direction
 x co-ordinate in chordwise direction
 y co-ordinate normal blade suction surface
 z co-ordinate in spanwise direction
 β_1 inlet flow angle with respect to cascade front

1. Introduction

The cascade originally was developed as a two-dimensional model that simulates the blade element flow of rotors and stators of turbomachines. Testing such a geometrically two-dimensional model in a wind tunnel, it is difficult or even impossible to obtain strictly two-dimensional flow conditions. Due to the finite dimensions of a wind tunnel the number of blade profiles and also the blade span is limited. Especially due to the limited span the adverse effect of the wind tunnel endwall boundary-layers on the flow field in the cascade model cannot be neglected. At least the near wall regions of the blade passages are influenced due to secondary flow effects.

Therefore most of the cascade experiments concentrate on the mid-span region, where secondary flow effects can be neglected and one can assume that blade pressure distribution, flow turning, and total pressure losses represent a two-dimensional or quasi three-dimensional flow field.

The adverse effect of the endwall boundary layers may increase, however, when the upstream velocity to the cascade becomes transonic and supersonic. Shock waves develop in the front and within the blade passages and interfere with the endwall boundary-layers eventually forcing local boundary-layer separations. Starting at these regions of strong interaction, disturbances can extend towards the wind tunnel center influencing the midspan flow field. In this paper such a phenomenon of shock wave endwall boundary-layer interaction and the resulting influence on the flow field in the cascade entrance region is described and discussed.

2. Test of a supersonic compressor cascade

The flow field in the entrance region of a cascade with supersonic inlet Mach numbers is characterized by a periodic pattern of bow shock waves, which are detached from the blade leading edges, and following expansion waves emanating from the front portions of the blades (Figure 1). The expansion waves, which are mainly

centered around the blade leading edges, cause a relatively rapid reduction of the shock strength in the inlet plane. Therefore the interaction of these oblique shocks with the wind tunnel endwall boundary layers usually can be neglected.

During a test series with a supersonic compressor cascade, that had a rather low blade aspect ratio of 0.9 (152.4 mm span, 170 mm chord) and thus a relatively thick profile leading edge ($t_{LE} = 0.85$ mm), some discrepancies appeared between the experimental and theoretical midspan suction surface Mach number distribution (Figure 2). The blade was designed for a supersonic inlet Mach number of 1.5 and should decelerate the flow to subsonic velocities. In order to reduce the Mach numbers incident to the first passage shock wave, the blade was designed with a negative suction surface camber along the cascade entrance portion. Thereby a relatively strong flow deceleration starts just at the blade leading edge and reduces the average Mach number at the passage entrance to a level less than the inlet Mach number. As to be seen in Figure 2 discrepancies occur between the analytical and measured blade suction surface Mach number distribution in the region from about 42 to 90 mm chord.

3. Inlet flow field analysis

In order to find out the reasons for the detected discrepancies, a test series was started, in which the flow field in the entrance region of the supersonic cascade was analysed in spanwise direction:

- 1) Oil streaklines on the blade suction surface (Figure 3) indicated some disturbances emanating from the blade leading edge endwall corner region traveling towards the blade center with an inclination of about 40 degrees to the tunnel walls. The gradients of the oil streakline pattern are greatest near the leading edge corner and attenuate towards the blade center. (The accumulation of oil behind 72% chord indicated a full turbulent boundary layer separation. It

should be mentioned here, that this photograph belongs to a test case that has a lower back pressure than that one shown in Figure 2).

- 2) A Laser-2-Focus (L2F) anemometer /1/ was used to obtain more information and some quantitative data of the detected phenomenon. Thereby the flow field near the blade suction surface was analysed in spanwise direction as illustrated in Figure 4 and 5. Basically the data were obtained from the region with the concave suction surface curvature, in which the flow is decelerated (pre-compressed): Therefore the velocity level of the spanwise Mach number profiles in Figure 5 drops down in chordwise direction. However, the spanwise profiles showed expansions and weak shock waves originating from the corner region, where the blade leading edge enters the endwall boundary-layer. The strength of these disturbances are strongest near the edge of the endwall boundary-layer and fade away gradually towards the blade center. The thickness of the incoming, undisturbed endwall boundary-layer was found to be around 13 mm.

4. Interpretation of results

It is assumed, that these disturbances are induced by a complex 3-dimensional interaction mechanism of the detached bow shock wave with the endwall boundary-layer. The sketches of the bow shock and the interaction region in Figures 1, 6, 7 and 8 may help to illustrate the phenomenon.

This complex fluid mechanical problem is not really understood. However, it is assumed that the strong branch of the bow shock induces a local endwall boundary layer separation ahead of the blade leading edge. From the local separation bubble on the tunnel sidewall/blade corner region, that may be formed like a horseshoe, a nearly centered expansion fan travels into the cascade flow passage (see section 2 in Figure 8 and Figure 9). The expansion finally is terminated by a weak oblique shock wave, the strength of which attenuates with increasing distance from the wall.

The local overexpansion and recompression emanating from the leading edge corner region shown in Figures 5 and 9 seems to be intensified by the type of the blade suction surface pressure distribution of the so-called pre-compression blade. This blade has a strong centered expansion around the leading edge, followed by a relatively strong recompression immediately downstream of the blade leading edge. The recompression region of the blade meets the recompression region emanating from the rear part of the endwall separation bubble (section 2 in Figure 8) so that the resulting shock strength increases slightly.

The dominant influence on the disturbances, however, comes from the leading edge thickness itself. The bluntness effect of the leading edge is responsible for the shock wave strength of the detached bow shock and the resulting local endwall boundary-layer separation. Very few information is available from other papers in the literature concerning this special type of three-dimensional shock boundary-layer interaction and its influence on the main flow field. Most of the papers /2, 3, 4/ treat the problem of sharp and blunt fin-induced interactions for very high freestream Mach numbers ($M \approx 2 - 3$) and they mainly concentrate on the local flow effects near the tunnel walls and not on the secondary induced effects which are reflected back into the mean flow field and back to the model.

5. Cascade with a blade aspect ratio of 1.8

A test series with a second type of blades, that had a smaller leading edge thickness and a nearly constant velocity distribution along the front portion of the suction surface (Figure 10) showed less disturbances in the corner region (Figures 11, 12, and 13). These tests were performed with a blade aspect ratio of 1.8 (85 mm chord) which is normally used in this wind tunnel. Fortunately the endwall disturbances fade away towards the tunnel center and an influence on the mid-span blade surface pressure distribution could not be recognized.

6. Conclusions

In principle these endwall disturbances cannot be avoided, however, by operating the tests with relatively large blade aspect ratios, the disturbances remain relatively weak and their influence on the mid-span performance can be neglected. How much the disturbances depend on the thickness of the incoming endwall boundary-layer cannot be answered yet, but some experimental results obtained from blunt fin-induced interactions /4/ indicate, that the properties in the interaction region primarily depend on the leading edge thickness and are only weakly affected by changes in incoming boundary-layer thickness.

7. References

- /1/ Schodl, R.: "A Laser-Two-Focus (L2F) Velocimeter for Automatic Flow Vector Measurements in the Rotating Components of Turbomachines", Trans. ASME, J. Fluid Eng., Vol. 102, No. 4, 1980.
- /2/ Kaufman II, L.G., Korkegi, R.H., Morton, L.C.: "Shock impingement caused by boundary-layer separation ahead of blunt fins." AIAA Journal, Vol. 11, No. 10, pp. 1363-1364, (Oct. 1973).
- /3/ Dolling, D.S, Cosad, C.D. and Bogdonoff, S.M.: "An examination of blunt fin-induced shock-wave turbulent boundary-layer interactions". AIAA Paper No. 79-0068 (Jan. 1979).
- /4/ Dolling, D.S.: "Comparison of sharp and blunt fin-induced shock-wave/turbulent boundary-layer interactions". AIAA Journal, Vol. 20, No 10, pp. 1385-1391 (Oct. 1982).

Table 1 Data of models and test condition

| | cascade 1 | cascade 2 |
|--|-------------------|------------------|
| blade aspect ratio | 0.9 | 1.8 |
| chord, l | 170 mm | 85 mm |
| span, b | 152.4 mm | 152.4 mm |
| leading edge thickness, t_{LE} | 0.85 mm | 0.59 mm |
| inlet Mach number | 1.5 | 1.51 |
| freestream Reynolds No. based on 100 mm | $1.51 \cdot 10^6$ | $1.6 \cdot 10^6$ |
| thickness of incoming boundary-layer, δ | ~ 13 mm | ~ 13 mm |
| ratio of leading edge thickness to boundary-layer thickness t_{LE}/δ | 0.065 | 0.045 |

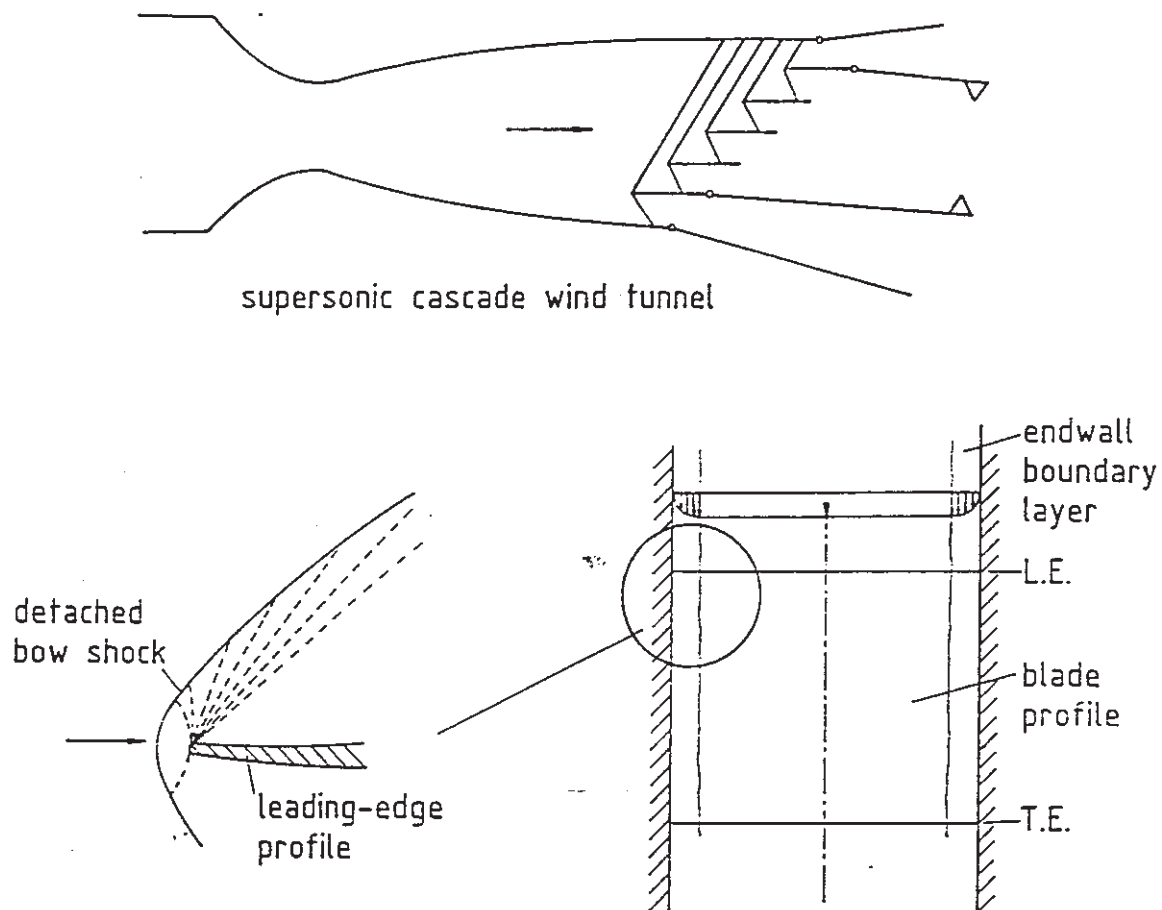
3. Figures

Fig. 1 Wind tunnel with a supersonic cascade and detached bow shocks ahead of the blade leading edges

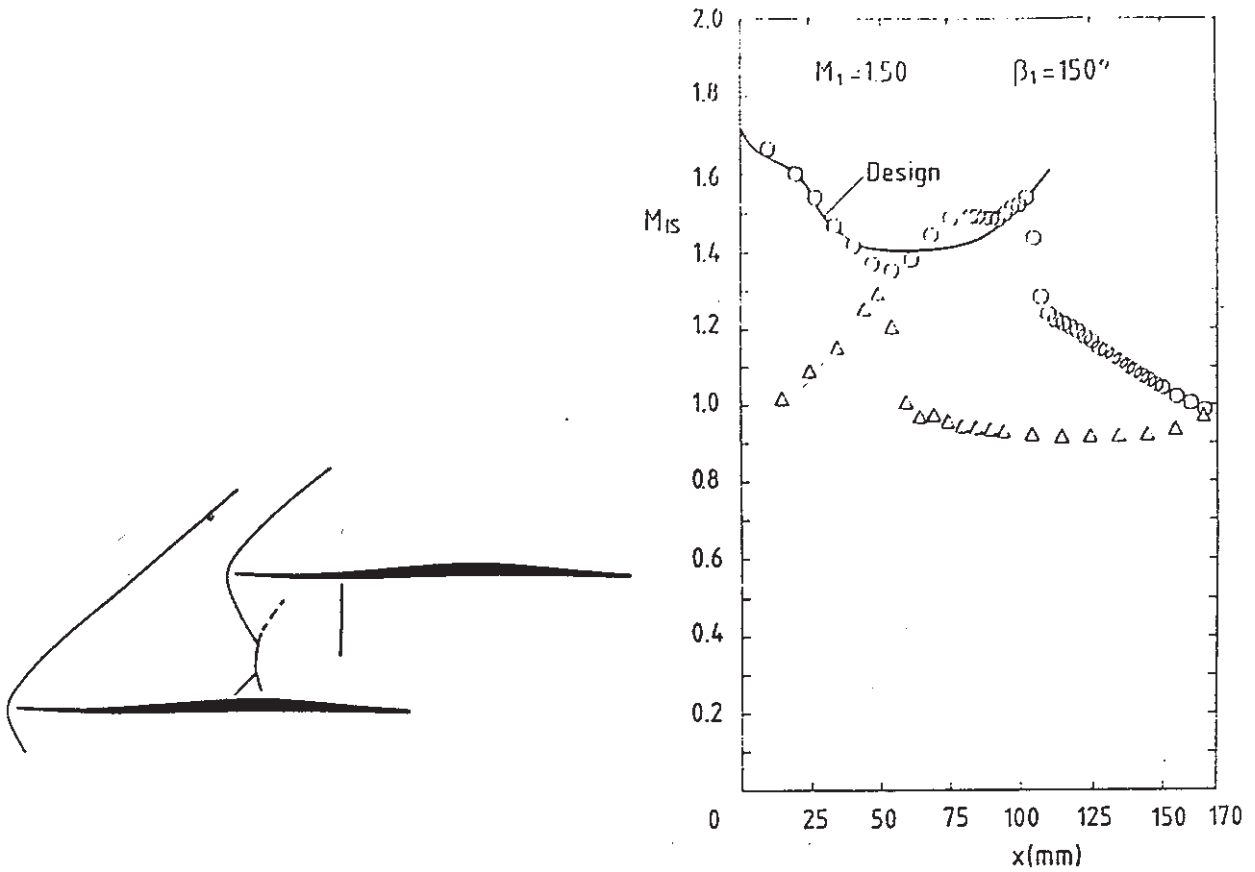


Fig. 2 Cascade with pre-compression profiles; measured blade Mach number distribution and comparison to design Mach number distribution along front portion, blade aspect ratio 0.9

Endwall disturbance

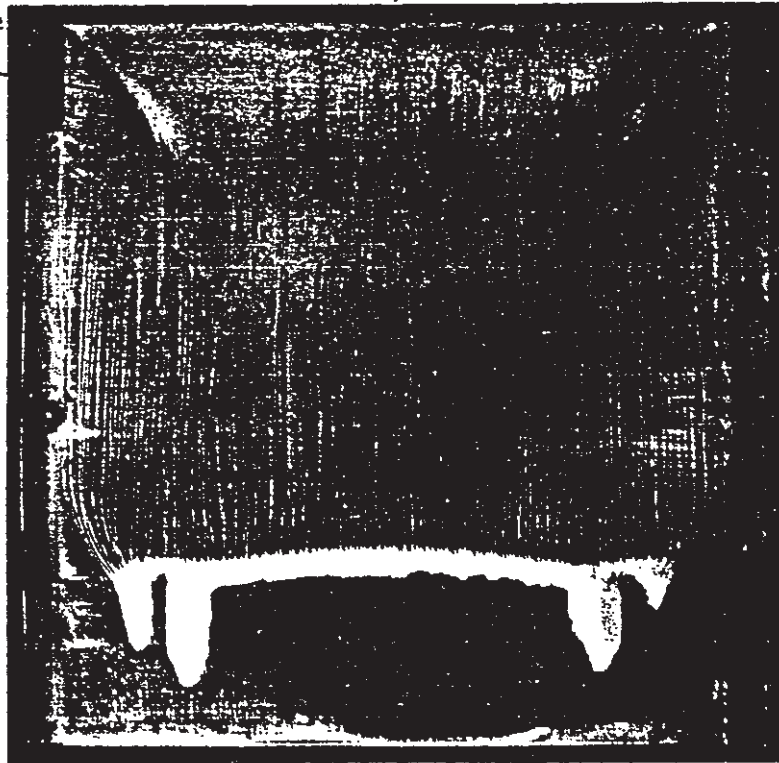


Fig. 3 Photograph of oil streaklines on the blade suction surface of a pre-compression profile indicating disturbances in the leading edge endwall corner region, $M_1 = 1.50$, $t_{LE} = 0.85$ mm

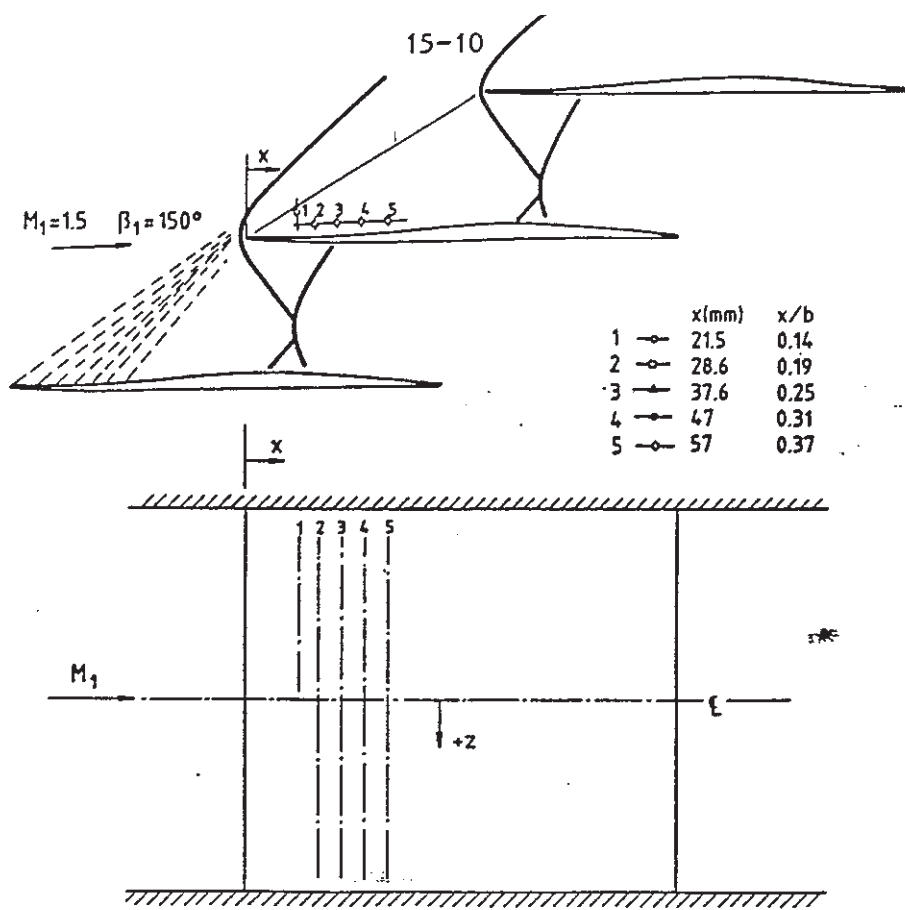


Fig. 4 Laser-2-Focus measurement planes in the entrance region of a pre-compression cascade

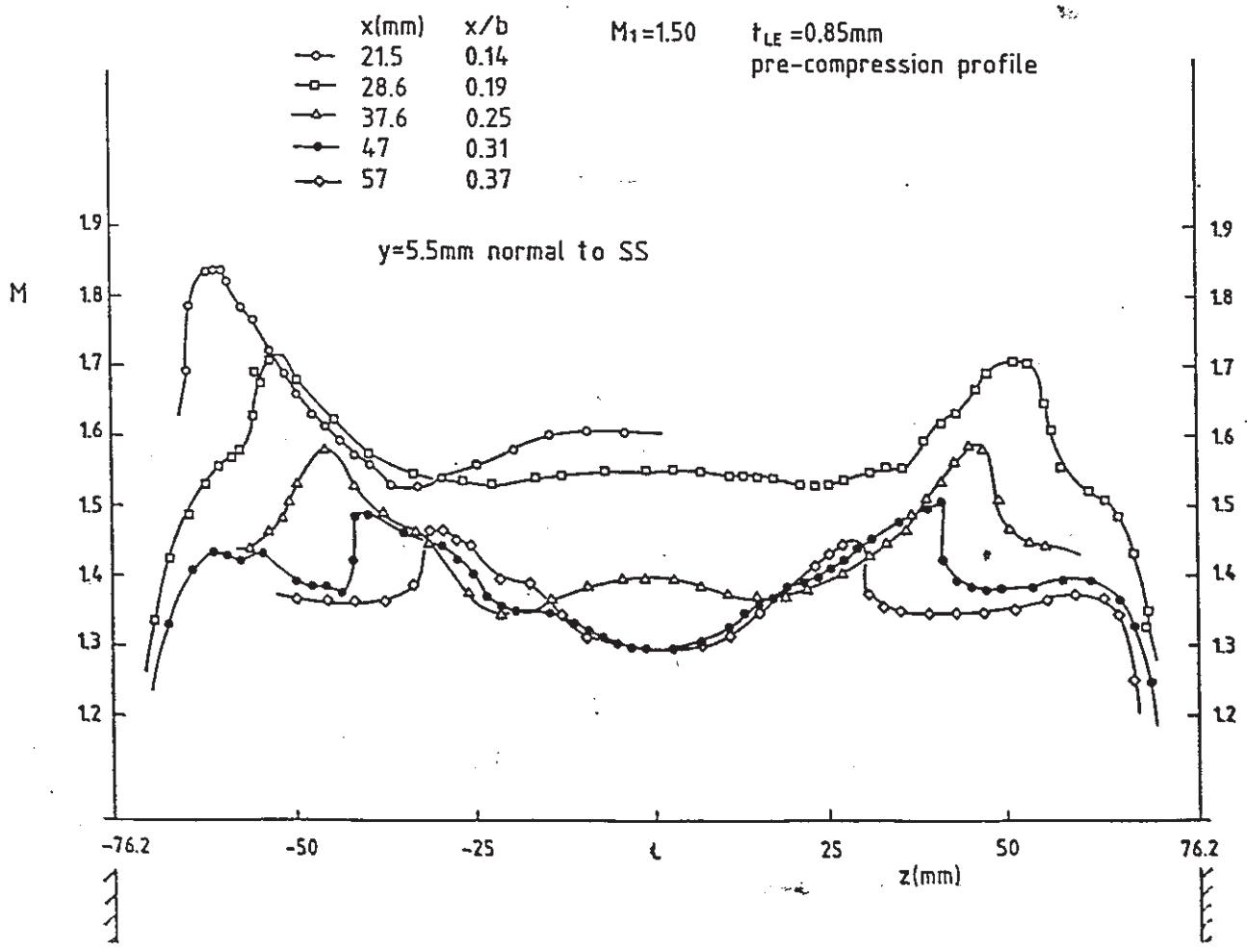


Fig. 5 Spanwise Mach number profiles in the front region of the cascade with pre-compression blades, blade aspect ratio 0.9

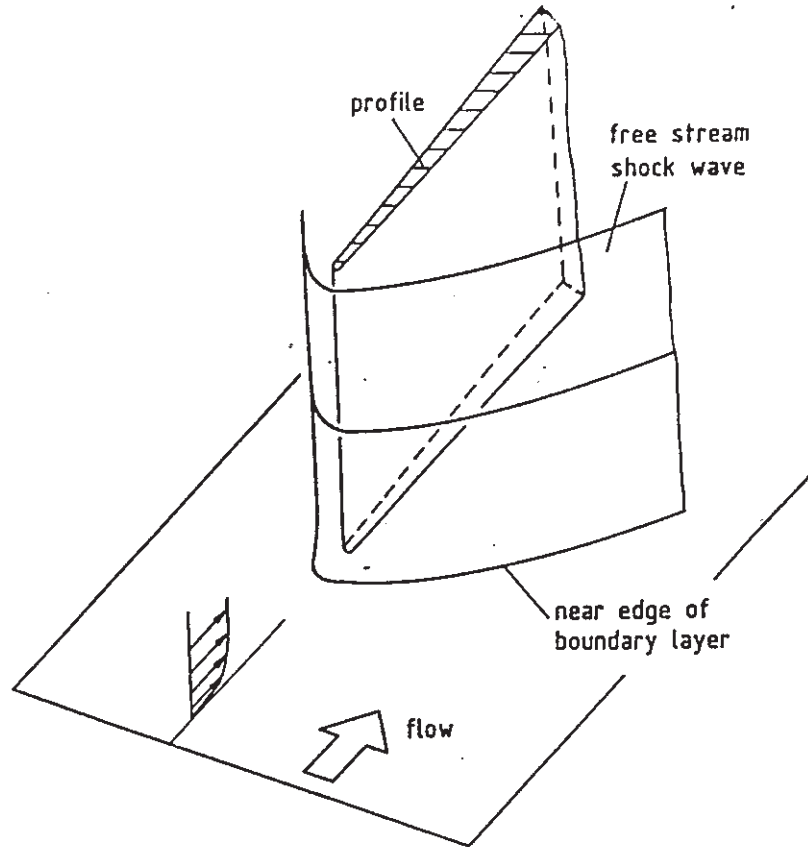


Fig. 6 Interaction of a detached bow shock wave with wind tunnel endwall boundary-layer

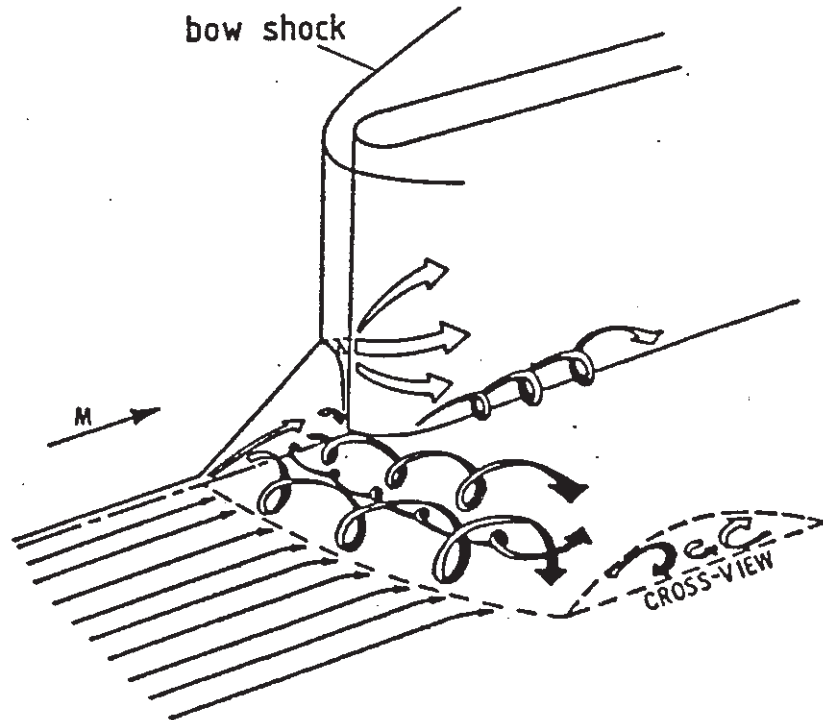


Fig. 7 Shock induced boundary-layer separation ahead of a blunt fin (after L.G. Kaufman)

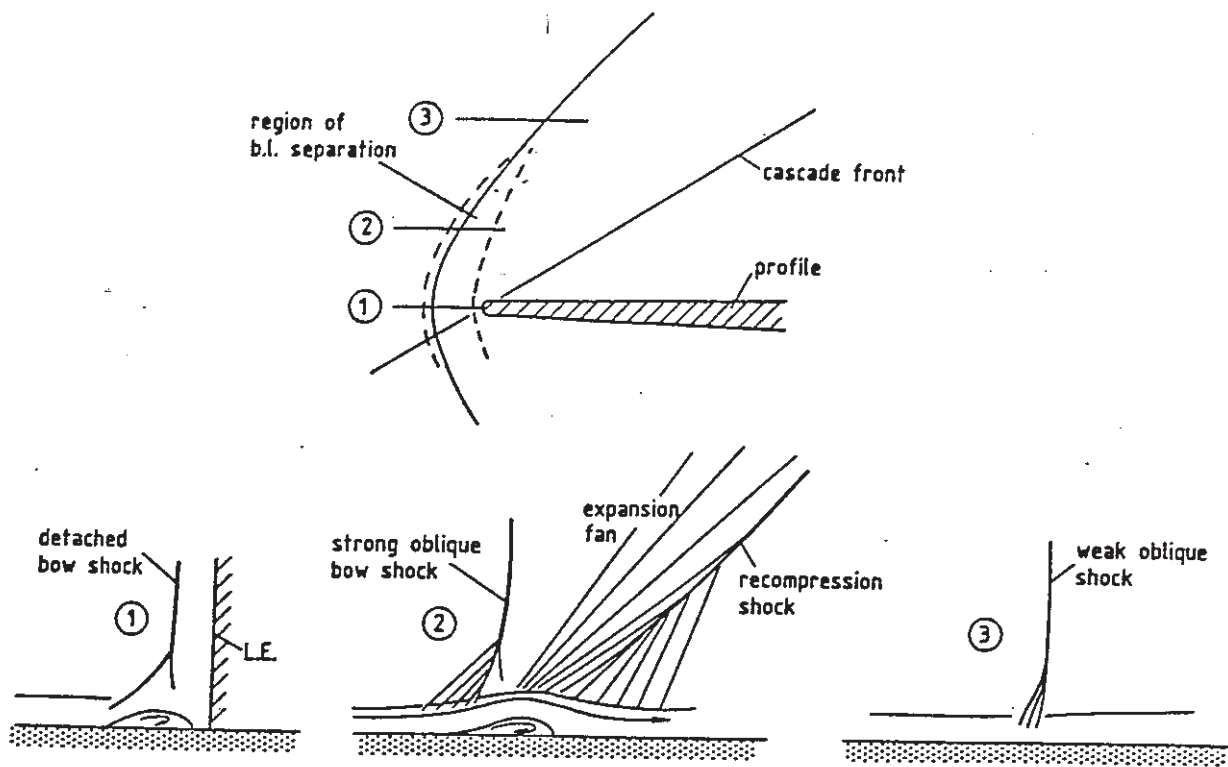


Fig. 8 Schematic representation of 3-dimensional shock wave endwall boundary-layer interaction near profile leading edge

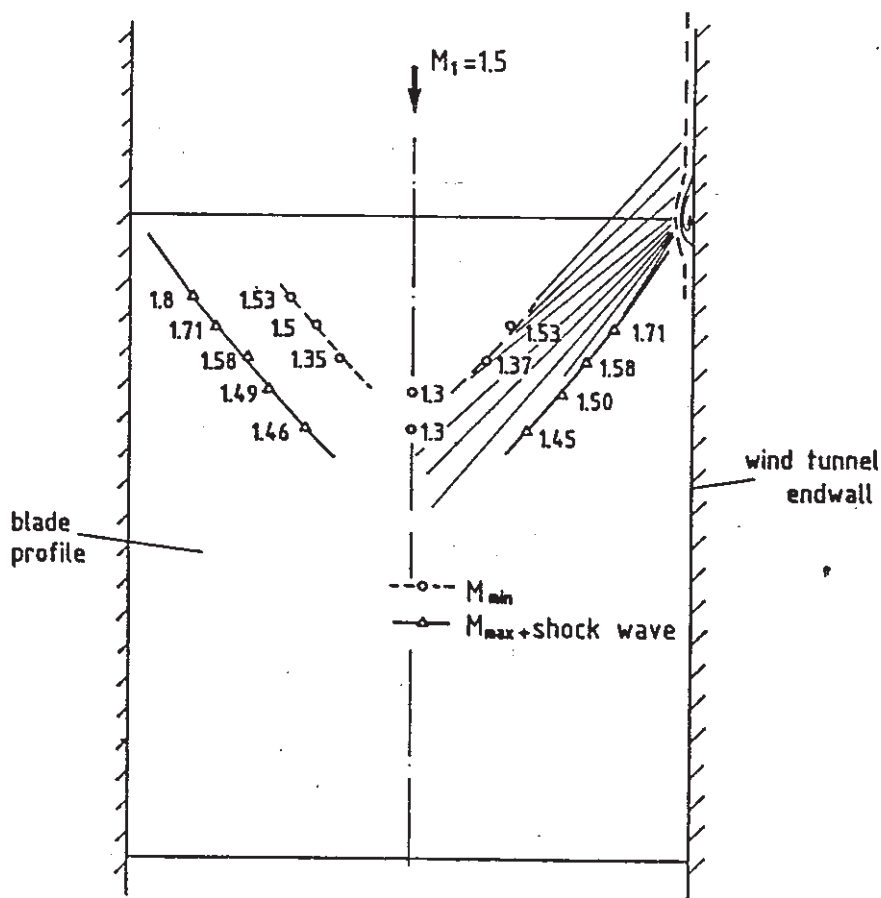


Fig. 9 Endwall disturbances in a plane about 5.5 mm above blade suction surface (Mach number data deduced from Fig. 5). Pre-compression profile, $t_{LE} = 0.85$ mm, blade aspect ratio 0.9

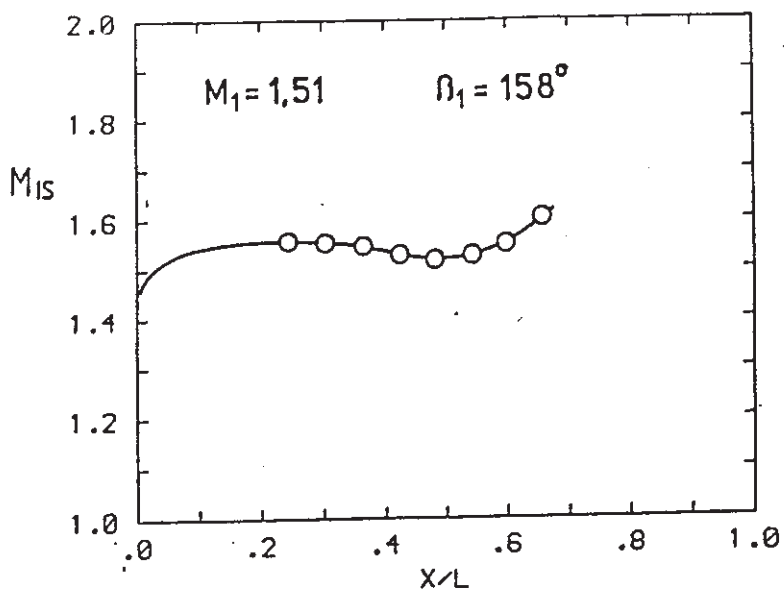


Fig. 10 Suction surface Mach number distribution along front portion of the blade with an aspect ratio of 1.8, $l=85$ mm

| | | | | |
|-----|----------------|-------|------------|------------------------|
| | $x(\text{mm})$ | x/b | $M_1=1.51$ | $t_{LE}=0.59\text{mm}$ |
| —□— | 16 | 0.10 | | |
| —○— | 24 | 0.16 | | |
| —△— | 40 | 0.26 | | |

$y=4\text{mm}$ normal to SS

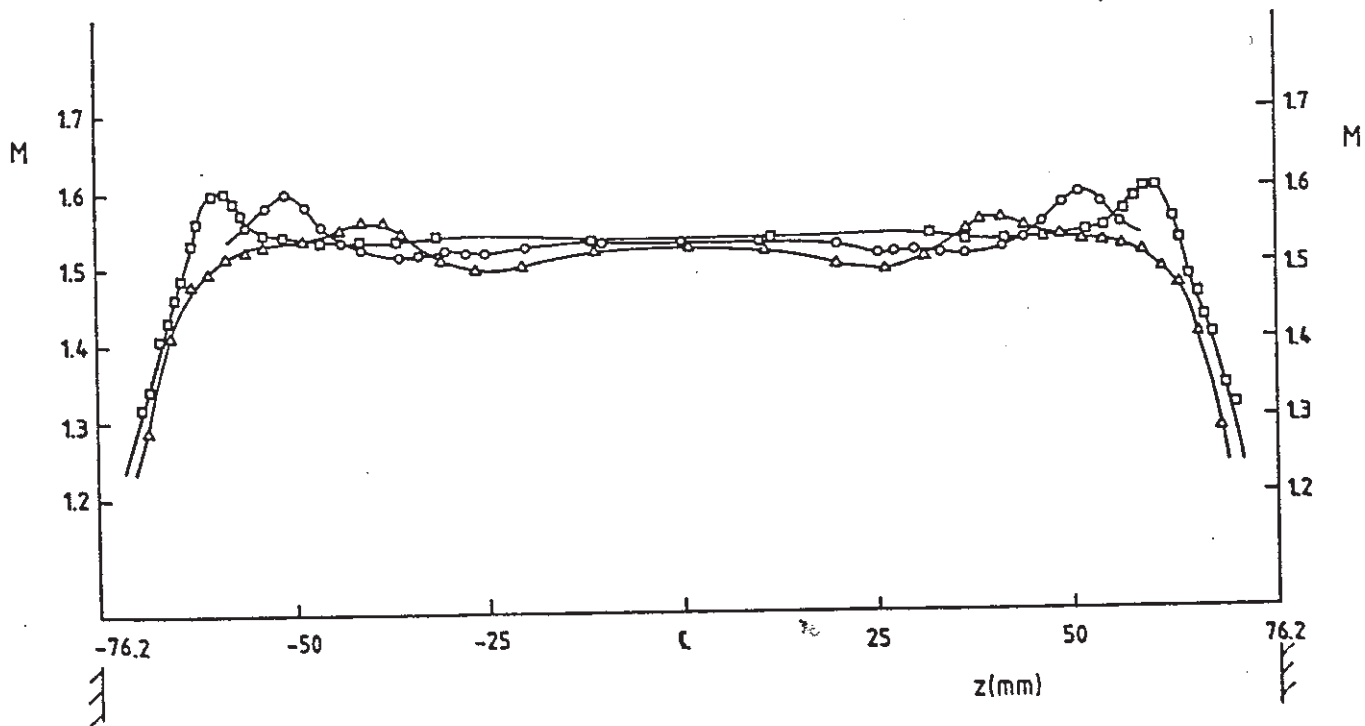


Fig. 11 Spanwise Mach number profiles in the front region of the blade with an aspect ratio of 1.8 and $t_{LE} = 0.59$ mm ($y = 4\text{mm}$ normal to blade suction surface)

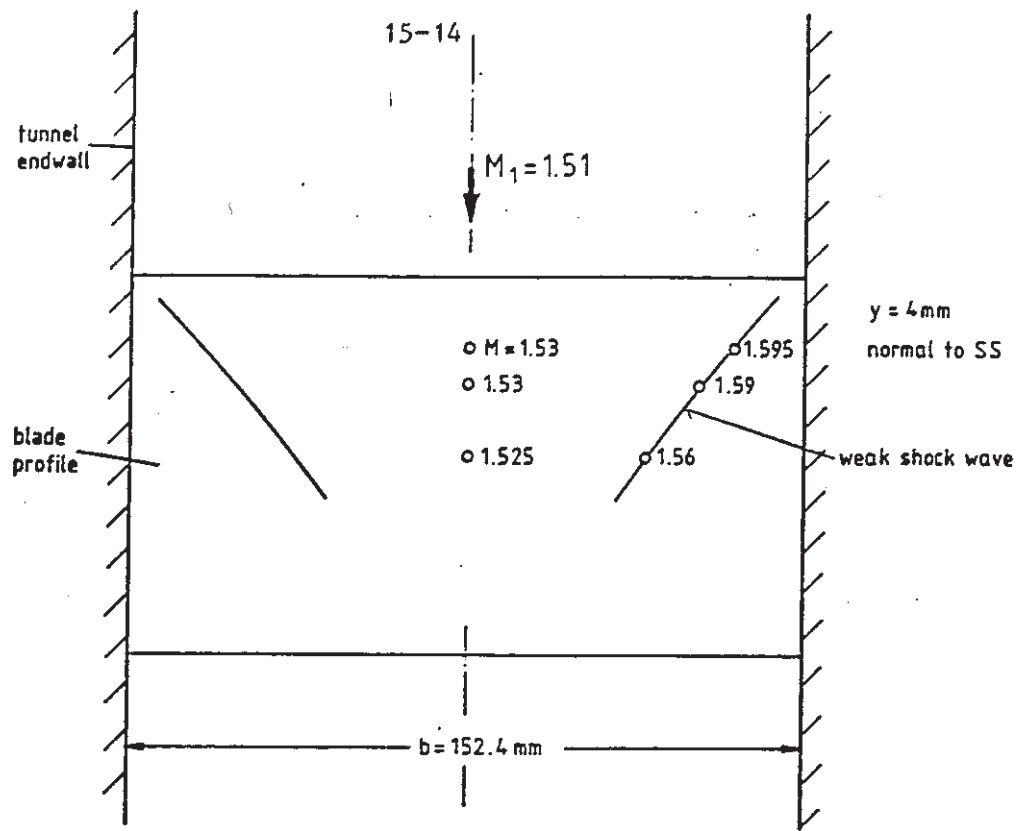


Fig. 12 Endwall disturbances in a plane about 4 mm above blade suction surface (data deduced from Fig. 11), $t_{LE} = 0.59$ mm, blade aspect ratio 1.8

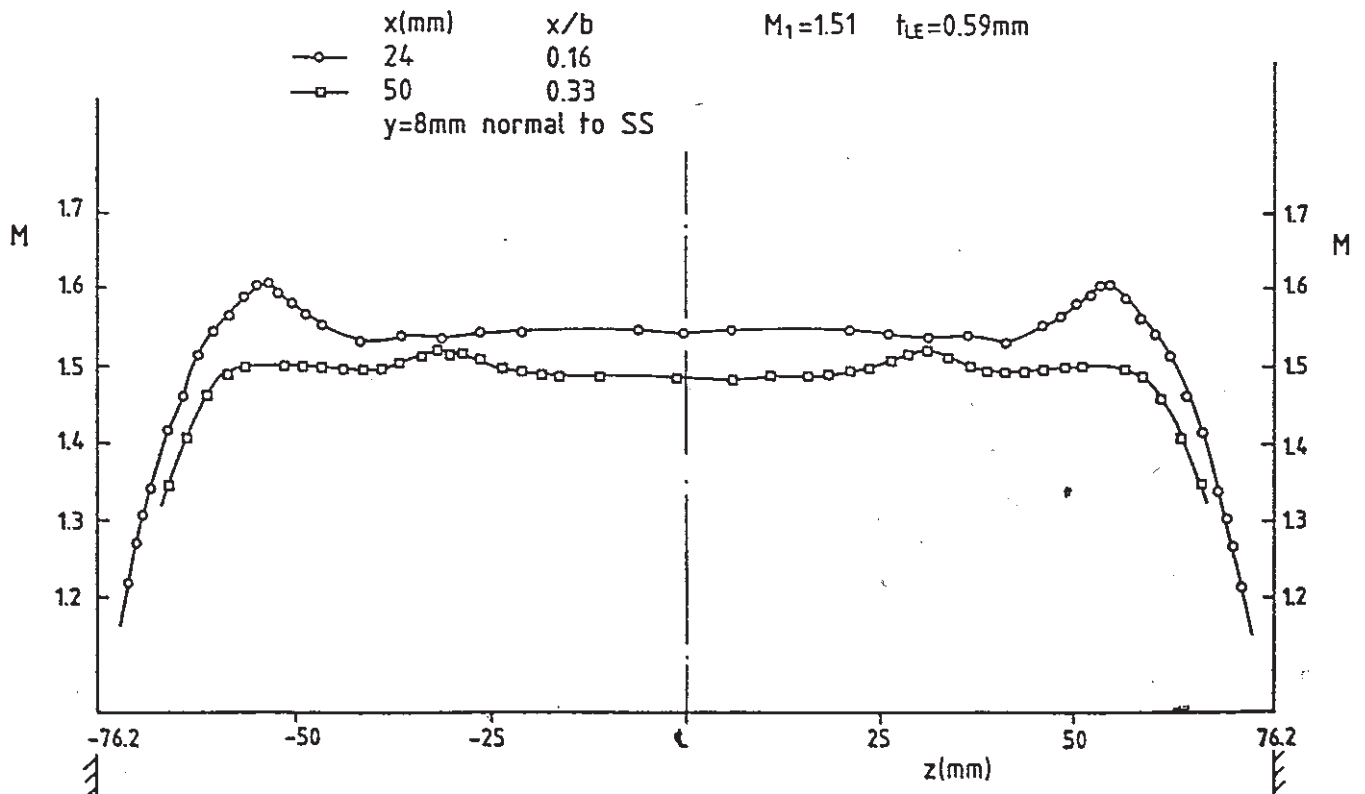


Fig. 13 Spanwise Mach number profiles in the front region of the blade with an aspect ratio of 1.8 and $t_{LE} = 0.59$ mm ($y = 8$ mm normal to blade suction surface)